Electrochemical Process and Phase Formation of Fe-Based Alloy Nanowires into Anodic Alumina Oxide

Tahir Mehmood[1], Aiman Mukhtar[1], Babar Shahzad Khan[2], Adnan Saeed[2], Waqar Ahmad[3], Wu kaiming[1,*]

[1] The State Key Laboratory of Refractories and Metallurgy, Hubei Province Key Laboratory of Systems Science in Metallurgical Process, International Research Institute for Steel Technology, Wuhan University of Science and Technology, Wuhan 430081, P. R. China
[2] Department of physics, Govt. College Women University, Sialkot, Punjab, Pakistan
[3] Wuhan National Laboratory for Optoelectronics, Huazhong University of Science and Technology, Wuhan 430074, P. R. China
[*] E-mail: tahir10621@yahoo.com, wukaiming@wust.edu.cn

The effect of deposition parameters on the phase formation and composition of Fe-Co alloy nanowires into nanopores of anodic alumina oxide membrane is considered by XRD, FE-SEM, TEM and EDX via electrochemical deposition technique. The deposited alloy nanowires are metastable fcc phase at – 4.0 V and at –2.0 V are stable hcp phase. These experimental results can be explained by the classic electrochemical nucleation theory. The formation of fcc crystals can be attributed to smaller critical clusters formed at a higher potential, lower deposition temperature and higher concentration of metal ions during electrochemical deposition process. The content of Fe inside nanowires increases with increasing potential, decreasing deposition temperature and increasing concentration of Fe ions. This can be verified by the polarization curves of depositing Fe and Co nanowires, where the current density ratio of Co to Fe at –2.0 V (0.79) is higher than that at –4.0 V (0.75).

1. INTRODUCTION

In last decade, an excessive deal of development has been made in the fabrication and characterization of numerous nanostructures with manageable morphology and properties, containing one dimensional structure such as nanotubes, nanorods and nanowires [1-3]. Quite a lot of studies have been reported on experimental conditions of forming fcc Co in electrodeposition at ambient

temperature. Huang et al. [4] considered allotropic phase conversion in bulk metallic cobalt by milling it within an inert gas atmosphere. An improved symmetry in the fcc structure (limited size) carried hcp to fcc transformation which supports its reliability. Development of a stable structure in a chemical reaction materializes by its nucleation followed through its rapid growth in an equilibrium state. The growth of a nanostructure, which is a natural, typical and usual process, occurs by means of lowering its whole energy as well as the entire energy of the system. For an example of slight critical volume, the Gibb's free energy is not dependent on a solo parameter of its radius r, as in the classical method, but on the real average spherical density profile [5].

Nevertheless, the synthesis of soft magnetic nanowires with requisite geometry and composition is quite challenging. Nanowires are used as the manufacturing materials for magnetic data storage, sound or gas sensors, biomedical materials, and for the fabrication of transistors and diodes for electronic systems. In recent times, much interest has been dedicated to synthesis Fe-Co nanowires owing to their application in magnetic recording devices and different kind of sensors [6]. Some recent studies have share out with the optimization of the direct current electrodeposition of Co based alloys with respect to several target factors. The effect of work function on growth of Fe and Co (individually) nanowires and complete understanding of the electrode reaction mechanism is described in our previous research work [7]. However Composition depth profile of these alloys appears to be a controversial issue. The standard equilibrium potentials of the iron and the cobalt metals are equal to _0.44 V and _0.23 versus SHE, respectively. Thus, it would be expected from thermodynamic considerations, that the preferential deposition is Co metal but for electrodeposition of the alloy, the less noble metal get preference in deposition to the nobler one. To solve this enigma, we have made an effort to discuss the deposition process of Fe-Co alloy nanowires and preferential growth via electrochemical deposition. The reasons for increasing content of Fe content in electrodeposition of binary alloy nanowires is discussed in details.

2. MATERIAL AND METHODS

Considerable attention has been attracted by electrochemical synthesis of metallic nanowires in the holes of porous membranes due to their magnetic, optical and electronic characteristics and their potential to be used in nanotechnological applications. Although different synthetic processes have been used to fabricate nanostructures, but porous alumina template process is one of the most widely and commonly employed method for fabricating different types of nanostructures owing to its easy fabrication. The idea of employing membrane as a template to fabricate metallic nanowires through electrodeposition is deemed as an alternative method to overcome the difficulty of fabricating fibrils having small diameter by lithographic process. Historically speaking, electrochemical synthesis technique was first developed by Possin to produce single metal wires of different characteristics. Later, his technique was improved by William and Giordano and metal wires of Au with 80 A in diameters were manufactured by them.

Anodic Aluminum Oxide (AAO) is a well-established nanotechnique for various research subjects, such as metallic nanowires, carbon nanotubes, quantum dots, and masks [8-10]. The structure of self-ordered anodized aluminum templates has been known to form during the transformation of aluminum into alumina by volume expansion and mechanical driving forces. When the volume expansion ratio peaks with the highest mechanical driving force, pores are unable to form under oxidation conditions. There are many factors that influence the ordered of the AAO template, e.g. voltage, temperature, concentration and type of electrolyte, purity of aluminum foil, and other electrochemical conditions [11, 12].

Anodization is the process in which the thickness of existing natural oxide layer on the surface increases when connected to positive terminal (anode) in an acidic solution. Before anodization, pretreatment of electrode is necessary to get the smooth and homogenous surface to large extent. This confirms an even surface of high quality with low contamination and low roughness, which makes the formation of pores for the subsequent electrodeposition of NWs more ideal. When the templates are not properly cleaned, samples tend to have defects that could impede the success of the process at later steps. For this purpose, pure aluminum (99.999%) foils were first degreased in acetone for 10 minutes and then annealed in a vacuum of 10^{-5} Torr at 500^{0}C for 5 h to get the homogenous structure.

Anodic Aluminum Oxide (AAO) is a well-established nano-technique for numerous research subjects, such as carbon nanotubes, masks, quantum dots, and metallic nanowires [8, 10]. There are several factors that have impact on the ordered of the AAO template, e.g. purity of aluminum foil, concentration and type of electrolyte, voltage, temperature, and electrochemical conditions [11-13]. Anodic alumina oxide template are prepared by anodization of aluminum foils in acid electrolytes containing bivalent or trivalent anions such as: phosphoric acid H_3PO_4 [12], sulphuric acid H_2SO_4 [13], or oxalic acid $(COOH)_2$ [14]. The different anodization conditions and obtained pore diameter are presented in the Table 1.

Two-step method first proposed by Masuda and Fukuda [15] is the best way to prepare plane and good quality membrane. The first anodization step includes a long-period anodization of pretreated high purity aluminum to form a porous alumina layer. In our case, the annealed aluminum foil is anodized at 2^{0}C under anodic voltage of 40 V in 0.3 M aqueous solution of oxalic acid $(H_2C_2O_4)$ for 6 hours, with the graphite plate as counter electrode.

Table 1. Anodizing processes for producing AAO templates with different pore size [16].

Electrolyte		Applied Voltage (V)	Temperature ($^{\circ}$C)	Pore Diameter
Composition	Concentration			
H_2SO_4	0.3 M	15-20	0$\pm$2	10-20 nm
$(COOH)_2$	0.3 M	40	0$\pm$2	40-50 nm
H_3PO_4	0.3 M	160-170	0$\pm$2	>150 nm

A shapeless alumina (Al_2O_3) porous film is formed after the first anodization step. To remove the formed alumina barrier layer the anodized aluminum films are dissolved in a mixed solution of phosphoric acid (6 wt%) and chromic acid (1.8 wt%) for 12 hours at 60 °C. Subsequent dissolution of

the porous alumina layer leads to a patterned aluminum substrate with ordered honeycomb pore arrangement attained during the first anodization process.

The ordered honeycomb formed in above mentioned treatment serve as the initial sites to form a highly ordered nanopore array in a second anodization step. To get more deep hexagonal and ordered honeycomb pores, aluminum foils were re-anodized under same conditions of first anodization step, but for 12 hours.

After the two step anodization, the aluminum from back side is removed in saturated $CuCl_2$ solution, and in a 5 wt% phosphoric acid solution at 40^0C alumina barrier layer was dissolved. The templates obtained by the above method have cylindrical and hexagonally arranged pores of about 50 nm in diameter and the length of the pore is about 65 μm .

In order to deposit metal nanowires into the pores of AAO templates, gold (Au) film is sputtered onto the back side of the AAO templates to serve as a working electrode by using (LEICA EM ACE 200). Figure 1 shows the the barrier layer and porous layes on aluminum foil of AAO template. Figure 2 gives front and top-view SEM image of AAO template, indicating that the pores on AAO template are hexagonally arranged and highly ordered with average diameter of about 50 nm.
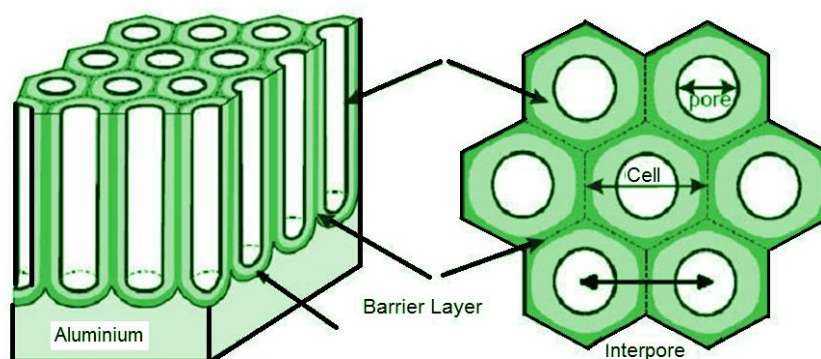

Figure 1. Schematic illustration of front and top view AAO templates showing the barrier layer and porous layes on aluminum foil [16].
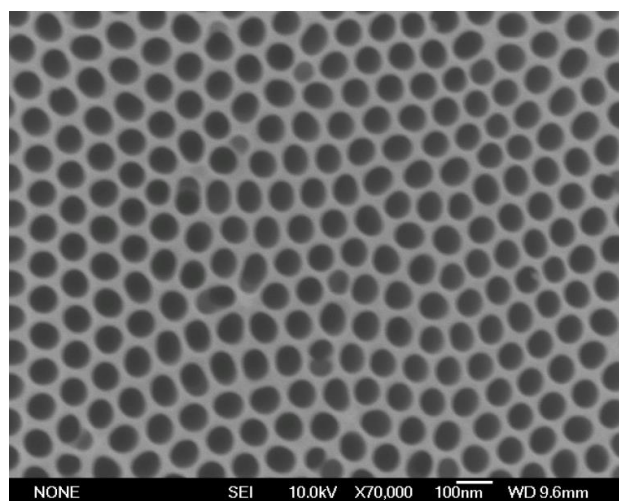

Figure 2. Homemade SEM image of AAO template prepared by two step anodization method

The electrolyte was $FeSO_4 \cdot 7H_2O$, $CoSO_4 \cdot 7H_2O$ with same concentration (50g/L each) and H_3BO_3 (40g/L) for deposition of alloy nanowires. The pH of the two as-prepared solutions was adjusted to 2.5 by adding 1M H_2SO_4 solution. Direct current electrodeposition was conducted in a three-electrode at room temprature. Direct current electrodeposition was conducted in a three-electrode. The Fe-Co alloy nanowires were analyzed were analyzed using XRD (X'Pert PRO MRD, PANalytical, Netherlands) with CuK$_\alpha$ radiation, using FE-SEM (NOVA 400 Nano) with EDS (Le350 PentaFETx-3) and transmission electron microscope (TEM, JEOL JEM-2010).

3. RESULTS

Figure 3 shows XRD patterns of Fe-Co alloy nanowires deposited at –2.0 V and –4.0 V. The XRD data of Figure 3 were collected from the top side of nanowires. The alloy nanowires deposited at –2.0 V have two peaks which can be fitted to the peak due to hcp (100) and hcp (002). The Fe-Co alloy nanowires deposited at –4.0 V have two peaks which can be attributed to fcc (111) and fcc (220). To further identify fcc phase we have done TEM for both samples.
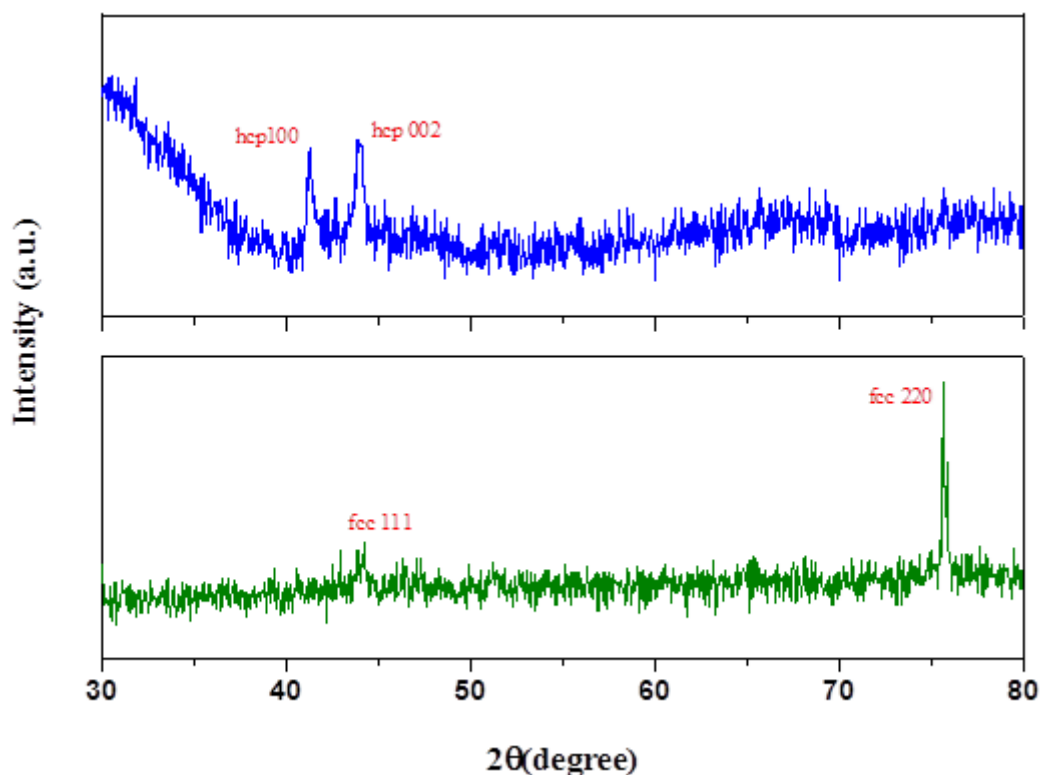

Figure 3. XRD patterns of Fe-Co alloy nanowires deposited at –2.0 V (blue) and –4.0 V (green) having equal concentration of both metals in electrolyte

Figure 4 shows SEM images and EDX results (table)   of the Fe-Co alloy nanowires deposited at –2.0 V and Fe-Co alloy nanowires deposited at –4.0 V. The compositions of Fe and Co were measured by using EDX at four random points for each sample and are listed in table below. The averaged compositions of Fe and Co are 50.74% and 49.26% in alloy nanowire deposited at –2.0 V

and the averaged compositions of Fe and Co in alloy nanowire deposited at –4.0 V are 53.57% and 47.43%.
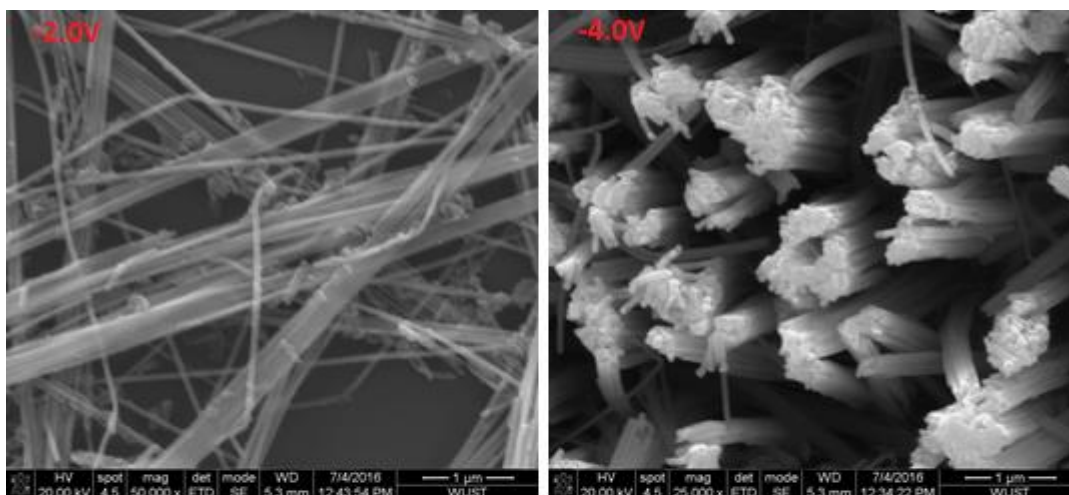
alloy (-2.0V)		alloy (-4.0V)	
Fe(at.%)	Co(at.%)	Fe(at.%)	Co(at.%)
50.69	49.31	53.7	47.3
50.85	49.15	53.83	47.17
50.87	49.13	53.66	47.34
50.55	49.45	53.09	47.91

Figure 4. SEM images and EDX results (table)   of the Fe-Co alloy nanowires deposited at –2.0 V and Fe-Co alloy nanowires deposited at –4.0 V

Moreover, the diameter of the alloy nanowires (~50nm) is the same as that of the pores of AAO template (~50nm), indicating that the nanopores of the AAO template were fully filled with alloy ions during electrodeposition.

TEM observations were made on the Alloy nanowires deposited at -2.0 and -4.0V in order to identify the phase of alloy. Figure 5 gives the TEM images and electron diffraction pattern of a Fe- Co nanowire deposited at -2.0 and -4.0V. The observed electron diffraction pattern is the same as the standard hcp crystal diffraction pattern in figure 5(a) and the same as the standard fcc crystal diffraction pattern in figure 5(b). Moreover, for alloy deposited at -4.0V, the observed ratio of the spot spacing of L to M (1.152) is in agreement with the ratio ($2/\sqrt{3} = 1.155$) in the standard diffraction pattern. Therefore, we believe that the Fe-Co nanowires deposited at high potential are an fcc phase.
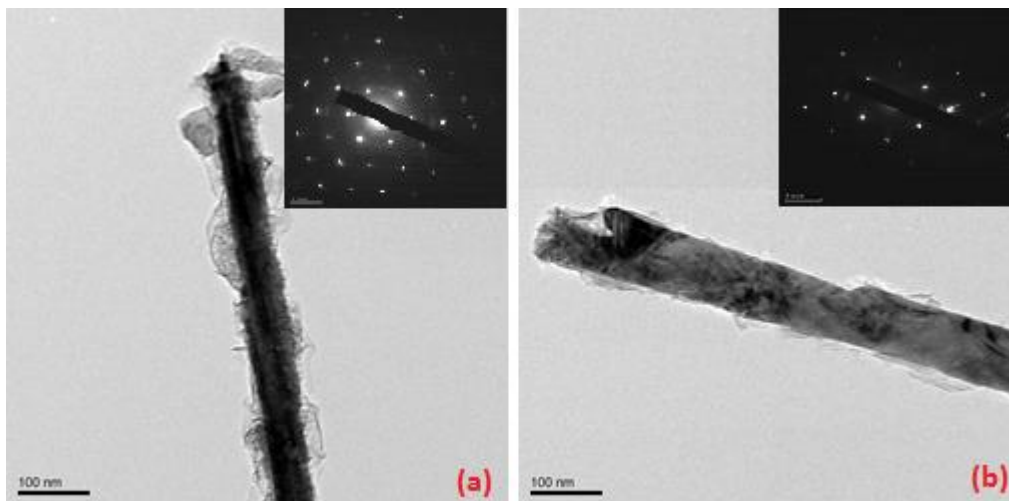
Figure 5. TEM images of Fe-Co alloy nanowires deposited (a) at -2.0 (relevant ED pattern inset) and (b) at -4.0V (relevant ED pattern inset)

In order to explain the effect of potential on the composition of alloy nanowires, the polarization curves of depositing Fe and Co nanowires having phosphate solutions with same deposition parameters were measured at a scanning rate of 0.1 mV/s respectively, as shown in figure 6.
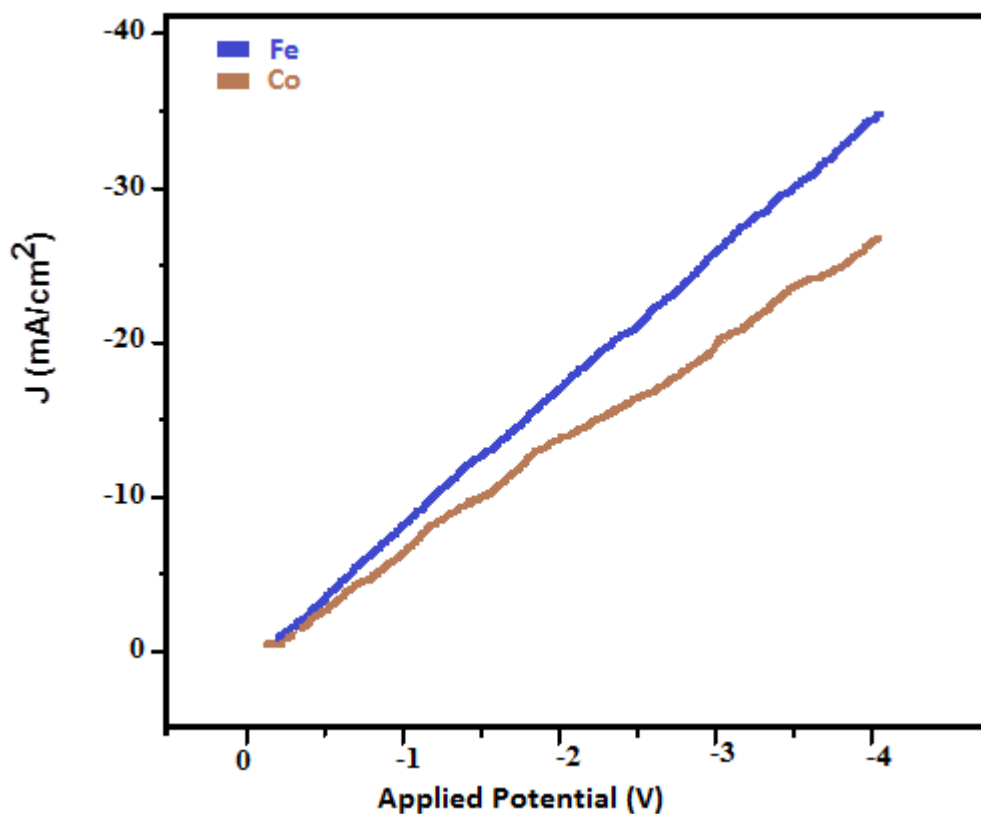

Figure 6. Polarization curves (scan rate 0.1mV/s) of depositing Fe and Co nanowires with same deposition parameters

The current density of depositing Fe nanowires increases more rapidly with applied potential than the current density of depositing Co nanowires. This current density relation is already discussed in our previous work [7].The current density ratio of Co to Fe was determined to be 0.79 at –2.0 V and 0.75 at –4.0 V.

4. DISCUSSION

The electrocrystallisation process of depositing metal atoms at the cathode from the bath containing Fe and Co ions involves the transfer of ions from bulk solution to the solution cathode interface which subsequently gets adsorbed on the cathode surface. After complete charge transfer from adsorbed ions, an alloy ad-atom forms on the cathode surface that diffuses to a vacant lattice site via nucleation and growth mechanism [17]. In this mechanism, the first step is a mass-transport process and hence it is controlled by the diameter and length of the pores in the AAO template. The mass transport within the nanopores is limited by diffusion[18].

In an electrolyte the mass transfer of ions takes place by three principal mechanisms: a) Diffusion, b) Migration, and c) Convection. Diffusion is the process by which matter moves due to random particle (ion, atom or molecule) motion. Diffusion took place from higher concentration to lower concentration, as the ionic concentration in bulk is higher than that of the electrode surface [Fontana's classical model], therefore diffusion of cations is towards electrode surface. Migration is due to the strong electric field which causes the potential gradient in the solution, and convection is due to the motion of fluid, which is influenced by the velocity and concentration of ions in the solution. Generally in an electrochemical cell when mass transfer is considered for the steady state, then coupled mass transfer process "Ambipolar diffusion" (diffusion flux and migration flux)[19] is taken into account. For Ambipolar diffusion, the rate of mass transfer or the total molar flux is the sum of the rates of ionic diffusion, given by Fick's law, and of ionic migration, with the ionic mobility given by the Nernst-Einstein relation between ionic mobility B and molecular diffusivity D [20].

$$\emptyset = \emptyset_D + \emptyset_M$$

$$\emptyset = -D\frac{dC}{dx} - CB\frac{dU}{dx}$$

And

$$B = \frac{F}{RT}D$$

Where $\emptyset$ is the total flux in x direction depending upon the diffusion flux $\emptyset_D$ and migration flux $\emptyset_M$, D the diffusion coefficient, C the concentration of ions in the solution, dC/dx the concentration gradient, and dU/dx is the potential gradient. As discussed above the molar flux is due to strong electric field, and the diffusion flux due to concentration gradient. In the following we

explain how these fluxes influence the current density and as a result, phase transformation of depositing alloy nanowires occur.

The total current density for the mass transfer can be defined by Nernst-Plank-Faraday equation[21] as,

$$i = zF \left[-D\frac{dC}{dx} - CB\frac{dU}{dx} \right]$$

Where z is the valence of metal ions, and F the Faraday's constant. For the steady state processes, we can express the rate of migration as a function of current per unit area perpendicular to the direction of transfer[22],

$$\emptyset_M = \gamma \frac{I}{zF}$$

Where γ is the transference number for the given species, and I is the current. In sufficient excess of inert electrolyte, the mobility of the metal ion is very low, its migration rate being dependent on the current and the transport number which is usually less than 0.5, so the migration of the ions may not be consider [22].

If ion's transfer by migration of the potential is negligible, then the dependence of current density or maximum rate of deposition can be described by Fick's law of diffusion as,

$$i_{lim} = zFD\frac{C}{\delta}$$

Here δ is the diffusion layer thickness. As ions are deposited within the pores of AAO template so the diffusion thickness can be considered as the length of the nanopore,

$$i_{lim} \propto C$$

From the equation, one can see that current density as a function of concentration. If $i < i_{lim}$ then the compact deposits are achieved. Whereas $i > i_{lim}$ leads to further charge of the double layer and finally, to other reduction processes.

Therefore, with increasing ion concentration of the electrolytes the current density must be increased in order to change the phase of deposits. One can see in our previous work [23], that the current density is different for different concentration. As the ionic concentration in the electrolyte become higher the current density also become higher and results in the faster growth of Co nanowires.

The crystalline metal nanowires will raise after the nucleus size surpasses the critical dimension N_c [24]. According to the classic electrochemical nucleation theory, the free energy of formation of a 3 dimension cluster of N adatoms, $\Delta G(N)$ is given by [25],

$$\Delta G(N) = -Nze\eta + bN^{\frac{2}{3}}$$

where z is the valence of hydrated metal ions, e is the elementary electric charge, η is the overpotential, b is the constant depending on the geometrical shape of the cluster.

The greater the N_c is, the more promising it is for a single crystal to develop from a formerly nucleated seed grain. Therefore, the critical dimension N_c for a 2D nucleus can be stated as [26],

$$N_c = bs \, \epsilon^2 / (Ze\eta)^2$$

Where z is the valence of hydrated metal ions, e is the elementary electric charge, b is the constant depending on the geometrical shape of the cluster, s is the area occupied by one atom on the surface of the nucleus and η is the overpotential which is defined as,

$$\eta = E(I) - E_0$$

Where E(I) is the exterior current induced potential and E_0 is the equilibrium potential of the electrode (the potential in the lack of the external current).

The following figure schematically shows the effect of applied potential on the sizes of nuclei. The nucleation sites are randomly distributed on Au surface. At very low potentials, the rate of producing ad-atoms on the surface is extremely low and each nucleus spreads over the entire surface before the next nucleus is produced while at high potential, the rate of producing ad-atoms on the surface is extremely high and large number of nucleus are produced in small size as shown in figure 7.
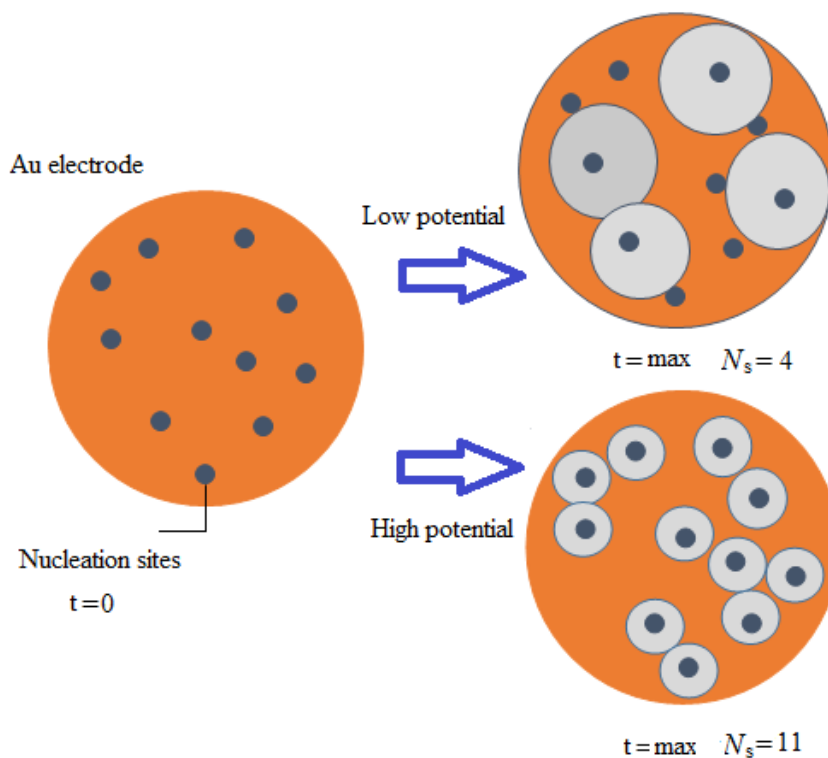

Figure 7. Schematic illustration of the influence of low potential (Ns =4) and high potential (Ns =11) on the sizes of nuclei

The larger N_s can represent the formation of smaller nuclei, favoring fcc structure due to the significant surface energy effect. Therefore, the Fe-Co alloy nanowires designed at –4.0 V are fcc phase while the Fe-Co alloy nanowires made at –2.0 V are hcp phase.

The compositions of alloy can depend on the polarization curves of depositing alloy metals [27]. The current density ratio of Co to Fe was determined to be 0.79 at –2.0 V and 0.75 at –4.0 V.

This specifies that the rate of depositing Fe atoms increases more quickly with increasing potential than that of depositing Co atoms because the current signifies the rate of generating metal ad-atoms.

In electrodeposition of metal, a metal ion M^{z+} is transferred from solution into the ionic metal lattice, meanwhile electrons are provided from the external electron source (power supply) to the electron gas of the metal M. Previously, we proposed four steps at atomic-level for the growth of metal nanowires [28]. In the first step the hydrated metal ions in an aqueous solution diffuse on the metal surface and then adsorbed on the surface. When an adsorbed hydrated metal ion captures electrons from the surface by quantum-mechanical tunneling, the metal ion is neutralized. The dehydration involves valence electrons tunneling to hydrated metal ions [28], leading to neutralization of the hydrated metal ions. The neutral metal atoms are adsorbed on the surface and then diffuse to surface sites (such as kink site) where they incorporate into the metal lattice, thus leading to the growth [28]. Therefore, the growth rate is related by the dehydration [28]. The diffusion of ions can be explained by Fick's law of diffusion. The current density of these hydrated metal ions directly relates with the presence of ions within the solution. Higher the concentration is, higher will be the current density. At constant deposition potential, this makes more ions available for deposition[18]. When there is accesses number of hydrated metal ions available for diffusion, then there is possibility that more valence electrons will tunnel through the barrier, result in to the higher current density and further leads to faster growth of alloy nanowires.

When electrodeposition originates, nucleation must arise. This situation is just related to the nucleation which happens in a supersaturated solution. Here an ion go into the diffusion layer, dehydrated, and after discharging it must diffuses and ultimately form a nucleus by linking other ad-atoms. The nucleation rate depends on the average number of critical clusters (n) and the diffusion of molecules to the cluster (β), is given by the equation,

$$I = n\beta$$

The average population of the critical nuclei is given by the relation,

$$n \propto exp(-\Delta G / k_B T)$$

Where ΔG is the critical free energy, T is the temperature, and k_B is the Boltzmann constant. The number of clusters increases with temperature. The crystal structure of Co nucleus can depend on the size. When the size of a Co nucleus is very small, the fcc phase can be thermodynamically more stable than the hcp phase due to the significant surface effect. Many researches confirmed by experimental observations that Co particles with small sizes are fcc phase [29-32]. From the relation, the nucleation probability will be high if we increase the temperature of electrolyte. On the higher nucleation rate, the size of the nucleus is small which results in the hcp phase as discussed above. The same phenomenon is seen in our case, higher temperature causes the higher nucleation rate result into hcp phase and lower temperature favor the smaller nuclei to form fcc Co. We intensely believe that a larger size of Co nucleus favors an hcp structure of Fe-Co alloy while a smaller size of Co nucleus favors an fcc structure of Fe-Co alloy.

5. CONCLUSIONS

There are important and significant findings of our research work,

First and more imperative one is, the Fe-Co alloy nanowires deposited at –4.0 V are metastable fcc phase while the Fe-Co alloy nanowires deposited at –2.0 V are stable hcp phase. The formation of Fe-Co fcc alloy nanowires can be credited to smaller critical clusters formed at the high potential, low deposition temperature and higher metal ion concentration. Second, higher potential leads to an increase of the Fe content inside nanowires. This can be understood by the polarization curves of depositing Fe and Co nanowires. The current density ratio of Co to Fe is 0.79 at –2.0 V is larger than that (0.75) at –4.0 V and therefore the content of Fe in the alloy increases with potential.

References

1. T. Mehmood, B.S. Khan, A. Mukhtar, X. Chen, P. Yi, M. Tan, *Mater. Lett.,* 130 (2014) 256.
2. T. Mehmood, B.S. Khan, A. Mukhtar, M. Tan, *Int. J. Mate. Res.,* 106 (2015) 957.
3. T. Mehmood, A. Mukhtar, H.H. Wang, B.S. Khan, *Int. J. Mate. Res.,* 107 (2015) 283.
4. J. Huang, Y. Wu, and H. Ye, *Acta materialia.*, 44 (1996) 1211.
5. R. Ashoori, *Nature.*, 379 (1996) 413.
6. S. Thongmee, H.L. Pang, J.B. Yi, J. Ding, J.Y. Lin, L.H. Van, *Acta Materialia.*, 57 (2009) 2482.
7. T. Mehmood, A. Mukhtar, B.S. Khan, K. Wu, *Int. J. Electrochem. Sci.,* 11 (2016) 6423.
8. S.Z. Chu, S. Inoue, K. Wada, K. Kurashima, *Electrochim. Acta.*, 51 (2005) 820.
9. J. Xu, X. Zhang, F. Chen, T. Li, Y. Li, X. Tao, *Appl. Surf. Sci.,* 239 (2005) 320.
10. C.T. Wu, F.H. Ko, H.Y. Hwang, *Microelectron Eng.*, 83 (2006) 1567.
11. A. Saedi, M. Ghorbani, *Mater. Chem. Phys.*, 91 (2005) 417.
12. F. Li, L. Zhang, R.M. *Metzger. Chem. Mater.*, 10 (1998) 2470.
13. O. Jessensky, F. Müller, U. Gösele, *Appl. Phys. Lett.*, 72 (1998) 1173.
14. A.P Li, F. Müller, A. Birner, K. Nielsch, U. Gösele, *Adv. Mater.*, 11 (1999) 483.
15. H. Masuda, K. Fukuda, *Science.*, 268 (1995) 1466.
16. F. Nasirpouri. PhD Thesis, Sharif University of Technology., (2005).
17. M. Darques, L. Piraux, A. Encinas, P.B. Guillemaud, A. Popa, U. Ebels, *Appl. Phys. Lett.*, 86 (2005) 072508.
18. H. Schlörb, V. Haehnel, M.S. Khatri, A. Srivastav, A. Kumar, L. Schultz, *physica status solidi (b).,* 247 (2010) 2364.
19. U.R. Evans, London, UK., (1961).
20. G.H. Geiger, D.R. Poirier, *Addison-Wesley Publishing Company.*, (1973) 449.
21. N. Perez, *Kluwer Academic Publisher.*, (2004).
22. C.W. Tobias, M. Eisenberg, C.R. Wilke, *J. Electrochem. Soc.*, 99 (1952) 359C.
23. A. Mukhtar, T. Mehmood, B.S. Khan, M. Tan, *J. Cryst. Growth.,* 441 (2016) 26.
24. M. Tian, J. Wang, J. Kurtz, T.E. Mallouk, M.H.W. Chan, *Nano Letters.,* 3 (2003) 919.
25. V.A. Isaev, O.V. Grishenkova, *Electrochemistry Communications.*, 3 (2001) 500.
26. J. Amblard, M. Froment, G. Maurin, N. Spyrellis, E.T. Souteyrand, *Electrochimica Acta.,* 28 (1983) 909.
27. P. Milan, M. Schlesinger, Fundamentals of Electrochemical Deposition, Wiley, New York., (1998).
28. M. Tan, X. Chen, *J. Electrochem. Soc.,* 159 (2012) K15.
29. A.R. Troiano, J.L. Tokich, *Trans. Metall. Soc.* AIME., 195 (1948) 728.
30. E.A. Owen, D.M. Jones, *Proc. R. Soc. London Ser. B.*, 67 (1954) 456.
31. K. Kimoto, Y. Kamiya, M. Nonoyama, R. Ueda, *Jpn. J. Appl. Phys.*, 2 (1963) 702.

32. S. Gangopadhyay, G.C. Hadjipanayis, C.M. Sorensen, K.J. Klabunde, *IEEE Trans. Magn.*, 28 (1992) 3174.